

# PH-GCN: Person Re-identification with Part-based Hierarchical Graph Convolutional Network

Bo Jiang, Xixi Wang, and Bin Luo

*Abstract*—The person re-identification (Re-ID) task requires to robustly extract feature representations for person images. Recently, part-based representation models have been widely studied for extracting the more compact and robust feature representations for person images to improve person Re-ID results. However, existing part-based representation models mostly extract the features of different parts independently which ignore the relationship information between different parts. To overcome this limitation, in this paper we propose a novel deep learning framework, named Part-based Hierarchical Graph Convolutional Network (PH-GCN) for person Re-ID problem. Given a person image, PH-GCN first constructs a hierarchical graph to represent the pairwise relationships among different parts. Then, both local and global feature learning are performed by the messages passing in PH-GCN, which takes other nodes information into account for part feature representation. Finally, a perceptron layer is adopted for the final person part label prediction and re-identification. The proposed framework provides a general solution that integrates *local, global* and *structural* feature learning simultaneously in a unified end-to-end network. Extensive experiments on several benchmark datasets demonstrate the effectiveness of the proposed PH-GCN based Re-ID approach.

## I. INTRODUCTION

Person re-identification (Re-ID) is an active research problem in computer vision [1], [2], [3], [4], [5], [6], [7], [8]. Many of existing Re-ID methods adopt a person classification framework which aims to determine the label of an input person image by using a classifier trained on the training samples [1], [9], [10], [2], [5], [11]. Although recent years have witnessed rapid advancements in person Re-ID, it is still a challenging task partly due to large changes of person appearance caused by variety of factors, such as pose, illumination, deformation and occlusion.

One main issue for Re-ID problem is to develop a compact and robust feature representation for person images. Recently, part-based methods have been widely studied and verified beneficially to person Re-ID task [12], [9], [13], [11], [1], [14], [15]. These methods generally conduct feature representation on part-level and thus can extract both local and global discriminative representations for person image. In particular, deeply-learned features have been verified stronger discriminative ability, especially when aggregated from deeply-learned part features [9], [12], [11], [15], [16]. For example, Zhao *et al.* [12] develop a human part-aligned representation for Re-ID. Sun *et al.* [11] propose Part-based Convolutional Baseline (PCB) for learning part-level features. Wei *et al.* [14] propose

Global-Local-Alignment descriptor (GLAD) to leverage both local and global cues. Zheng *et al.* [15] design a new coarse-fine pyramid model to conduct local and global representation.

**Motivation.** The above existing person Re-ID models mostly extract the features of different person parts independently which ignore the inherent spatial relationship information among different parts. Such spatial relationships are usually represented in the form of graphs. Recently, graph convolutional networks (GCNs) have draw increasing attention due to their ability of generalizing neural networks for data with graph structures [17], [18], [19], [20], [21]. GCNs aim to propagate messages on a graph structure. After message passing on the graph, the final node representations are obtained from their own as well as the information of their neighboring nodes, which thus can naturally incorporate the contextual information for node representations. Also, GCNs incorporate graph computation into the neural networks learning to make the training end-to-end, which can be naturally incorporated into some other deep learning frameworks. Motivated by these, in this paper we propose a novel Part-based Hierarchical Graph Convolutional Network (PH-GCN) for person image representation and Re-ID task. PH-GCN aims to learn a context-aware representation for each person part that incorporates the geometrical structure information among parts while maintains the unary appearance feature of each part. PH-GCN exploits the inherent relationships of parts effectively, and thus is robust to part noises and/or corruptions.

Overall, the main contributions of this paper are summarized as follows.

- We propose a novel deeply-learned and context-aware part feature extraction and learning model for person Re-ID. We show that the proposed representation has much higher discriminative ability than traditional part-based feature representations.
- We propose a novel Part-based Hierarchical Graph Convolutional Network (PH-GCN) learning framework for object representation. The proposed framework provides a general solution that integrates **local, global** and **structural** feature representation and learning simultaneously in a unified network.

Extensive experiments on several benchmark datasets demonstrate the effectiveness of the proposed PH-GCN method.

## II. RELATED WORKS

### A. Person re-identification

Many methods have been proposed for person Re-ID problem [1], [10], [2], [4], [6], [7], [8]. In this section, we briefly

Bo Jiang, Xixi Wang and Bin Luo are with the School of Computer Science and Technology, Anhui University, Hefei, China  
E-mail: jiangbo@ahu.edu.cn

review some recent related works that are also devoted to generate deeply-learned part features for Re-ID problem.

Ustinova *et al.* [8] propose a network architecture to learn a more effective embedding by performing bilinear pooling. Si *et al.* [2] propose to develop Dual Attention Matching network (DuATM) to learn context-aware feature sequences. Su *et al.* [9] propose Pose-driven Deep Convolutional (PDC) model, which aims to utilize the human part cues to alleviate the pose variations and thus learn robust features from both global image and local parts. Zhao *et al.* [12] propose a human part-aligned representation by detecting the human body regions and computing between the corresponding parts. Sun *et al.* [11] propose a strong convolution baseline method to further leverage a uniform partition strategy and thus learn a more compact representation for person Re-ID. Chen *et al.* [5] propose to combine CRF and deep neural network together and use multiple images to model the relationships between local similarity and global similarity. To further incorporate the global information, Wei *et al.* [14] propose Global-Local-Alignment Descriptor (GLAD) that explicitly leverages the local and global cues in human body to generate a discriminative and robust representation. Wang *et al.* [16] develop a feature learning strategy to integrate discriminative information by combining global and local information in different granularities. Zheng *et al.* [15] propose a new coarse-fine pyramid model to conduct local and global representation simultaneously.

### B. Graph convolutional network

Recently, graph convolutional neural networks (GCNs) have been demonstrated effectively for graph structure data representation and learning in machine learning area [17], [18], [19], [20], [21]. For example, Bruna *et al.* [22] propose a CNN-like neural architecture on graphs in Fourier domain. Defferrard *et al.* [20] propose to approximate the spectral filters by using recurrent Chebyshev polynomials. Kipf and Welling [18] further propose a simplified Graph Convolutional Network (GCN) based on the first-order approximation of spectral filters. Atwood and Towsley [23] propose Diffusion-Convolutional Neural Networks (DCNNs). Monti *et al.* [24] present mixture model CNNs (MoNet) to generalize CNN architecture on graphs. Veličković *et al.* [25] present Graph Attention Networks (GAT) by further designing an edge attention layer.

In addition, GCNs (or GNNs) have also been employed in computer vision tasks [26], [21], [27], [28]. For example, Michelle *et al.* [26] develop neural graph matching networks for few-shot 3D action recognition. Yan *et al.* [21] propose Spatial Temporal Graph Convolutional Network (ST-GCN) for skeleton-based action recognition. Qi *et al.* [27] propose a 3D graph neural network model for rgb-d semantic segmentation. Shen *et al.* [28] propose Deep Similarity-Guided Graph Neural Network (SGGNN) to explore the geometric relationships among different person images for person Re-ID. Different from SGGNN [28], here we exploit GCN for person feature representation. To the best of our knowledge, we are the first to employ GCN model to extract the context-aware part-based representation for person Re-ID task.

## III. PH-GCN MODEL

In this section, we propose our Part-based Hierarchical Graph Convolutional Network (PH-GCN) for person image representation and re-identification.

### A. Overview

Figure 1 shows the overall network module of PH-GCN which contains CNN based part feature extraction and part-based hierarchical graph construction, graph convolutional module and perceptron layer.

- **CNN based part feature extraction:** We utilize a deep CNN network module to extract the appearance feature for each part of person image.
- **Part-based hierarchical graph construction:** A hierarchical graph is constructed to encode the spatial relationships among different person parts.
- **Graph convolutional module:** We employ a graph convolutional network (GCN) architecture to extract the context-aware representations for person parts.
- **Perceptron layer:** A perceptron layer is defined for final Re-ID task.

In the following, we present the details of each module in our network, respectively.

### B. CNN based part feature extraction

For each person image  $I$ , we first use a pre-trained CNN model to extract convolutional feature descriptor for it. Then, we conduct three uniform partitions  $\mathcal{C}^{(p)}, p = 1, 2, 3$  on the conv-layer respectively to obtain global and local part-level features, as shown in Figure 1. In particular, we adopt ResNet50 [29] network and conduct partition on the 4th conv-layer. The parameters of ResNet50 network are pretrained on ImageNet [30]. Finally, we obtain a feature descriptor  $x_i^p$  for the  $i$ -th part in partition  $\mathcal{C}^{(p)}$  by using an average pooling strategy. We denote  $X^{(p)} = (x_1^p, x_2^p \cdots x_{n_p}^p) \in \mathbb{R}^{d \times n_p}, p = 1, 2, 3$  as the feature collections for different parts of image  $I$  in the following sections.

### C. Hierarchical part graph construction

Based on the above hierarchical partitions  $\mathcal{C}^{(p)}, p = 1, 2, 3$ , we construct a hierarchical graph  $G = (V, E)$  to represent the spatial and appearance relationships among different parts. In particular, we construct a three-layer graph whose nodes and edges are introduced below.

**Nodes.** A three-layer hierarchical graph  $G = (V, E)$  is constructed, where  $V = \{V^{(1)}, V^{(2)}, V^{(3)}\}$  with each  $V^{(p)}$  corresponding to the partition level  $\mathcal{C}^{(p)}, p = 1, 2, 3$ . Each node  $v_i^{(p)} \in V^{(p)}$  corresponds to a specific part which is assigned with a feature vector  $x_i^p$ , and there exist more nodes on the higher layers, i.e.,  $|V_3| > |V_2| > |V_1|$ . The higher layer contains more local information while the lower layer represents the global representation of person. We set  $|V_3|, |V_2|$  and  $|V_1|$  to 6, 3 and 1 respectively in our experiments.

**Edges.** Let  $E = \{E^w, E^b\}$  be the edge set, where  $E^w$  denotes the edges within each layer and  $E^b$  denotes the edges

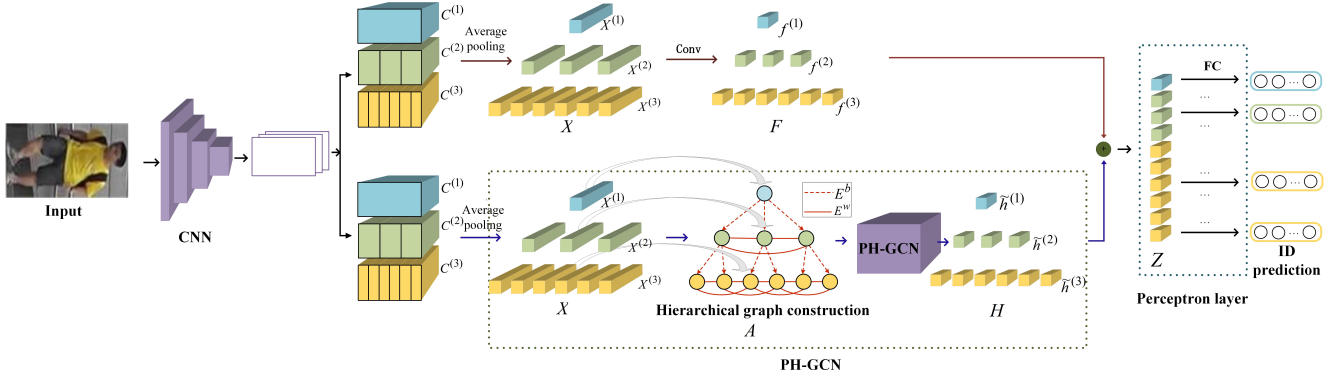


Fig. 1: Architecture of the proposed PH-GCN network for person Re-ID, which contains CNN based part feature extraction and hierarchical graph construction, graph convolutional module and perceptron layer.

existing between different layers. Specifically, in each intra-layer, an edge  $e_{ij} \in E^w$  exists between node  $v_i^p$  and  $v_j^p$  if they are either neighbour or they have common neighboring node. For different layers, an edge  $e_{ij}^{pq}, p \leq q$  exists between node  $v_i^p$  and  $v_j^q$  if the  $i$ -th part in  $p$ -layer involves the  $j$ -th part in  $q$ -layer. We compute the edge weight  $A_{ij}^{pq}$  for each edge as,

$$A_{ij}^{pq} = \exp\left(-\frac{\|x_i^p - x_j^q\|_2}{\delta}\right) \quad (1)$$

where  $\delta$  is a parameter.

#### D. Graph convolutional learning

As an extension of CNNs from regular grid to irregular graph, Graph Convolutional Networks (GCNs) [20], [18] have been widely studied for graph data representation and learning. Our GCN learning aims to extract a contextual and compact representation for each person part by exploring the representation information of its neighboring parts, which thus can exploit the more discriminative information for person Re-ID. GCN module contains several convolutional hidden layers that take a feature map matrix  $H^{(t)} \in \mathbb{R}^{N \times d_t}$  as the input and output a feature map  $H^{(t+1)} \in \mathbb{R}^{N \times d_{t+1}}$  by using a graph convolution operator. In general, we set  $d_{k+1} \leq d_k$ , and thus the convolution operation also provides a kind of low-dimensional representation for graph nodes.

Let  $X = [X^{(1)} \| X^{(2)} \| X^{(3)}]$  be the concatenation of  $X^{(p)}$ , where  $X^{(p)} = (x_1^p, x_2^p, \dots, x_{n_p}^p)$  be the extracted CNN feature collection of all parts. Let  $A$  be the whole adjacency matrix of the above hierarchical graph  $G(X, A)$ . We define  $A$  as

$$A = \begin{pmatrix} A^{11} & A^{12} & A^{13} \\ A^{21} & A^{22} & A^{23} \\ A^{31} & A^{32} & A^{33} \end{pmatrix}$$

where  $A^{pq}$  is defined in Eq.(1). Formally, given an input feature matrix  $X = H^{(0)} \in \mathbb{R}^{N \times d_0}$  and hierarchical graph  $A \in \mathbb{R}^{N \times N}$ . Similar to GCN [18], we propose to conduct the following layer-wise propagation as

$$H^{(t+1)} = \sigma[\epsilon \tilde{A} H^{(t)} + (1 - \epsilon) H^{(t)} \Theta^{(t)}] \quad (2)$$

where  $t = 0, 1, \dots, T-1$ .  $\sigma(\cdot)$  denotes an activation function. We define it as  $\sigma(\cdot) = \text{ReLU}(\cdot) = \max(0, \cdot)$ .  $\Theta =$

$\{\Theta^{(0)}, \Theta^{(2)} \dots \Theta^{(T-1)}\}$  denote the trainable weight matrices.  $\tilde{A}$  denotes the row-normalization of  $A$  [18]. Parameter  $\epsilon \in (0, 1)$  denotes the fraction of feature information that nodes receives from their neighbors.

#### E. Perceptron layer

In the final perceptron layer, we combine the visual appearance information and structure information together and then adopt a FC to predict part ID label.

For simplicity, we denote the final output feature map as  $\tilde{H} = H^{(T)} = \{\tilde{h}_1^{(1)}, \tilde{h}_1^{(2)}, \tilde{h}_2^{(2)}, \tilde{h}_3^{(2)}, \tilde{h}_1^{(3)} \dots \tilde{h}_6^{(3)}\}$ . Let  $F = \{f_1^{(1)}, f_1^{(2)}, f_2^{(2)}, f_3^{(2)}, f_1^{(3)} \dots f_6^{(3)}\}$  be the appearance feature extracted by CNN. First, we combine  $\tilde{H}$  and  $F$  into  $Z$  as,

$$z_i^{(p)} = \tilde{h}_i^{(p)} + \beta f_i^{(p)} \quad (3)$$

where  $\beta$  is a balancing parameter and  $z_i^{(p)}$  is a part component of  $Z$ . Then, for each part  $z_i^{(p)}$ , we adopt a FC layer to predict ID label of the corresponding person.

**Loss function.** For each part, we train a specific classifier by using the cross-entropy loss function  $\mathcal{L}_i^{(p)}$  [31]. The final overall loss function is designed as the aggregation of them,

$$\mathcal{L} = -\frac{1}{N} \sum_p \sum_i \mathcal{L}_i^{(p)} \quad (4)$$

where  $N$  is the number of parts.

## IV. EXPERIMENTS

To verify the effectiveness of the proposed PH-GCN method, we conduct experiments on three benchmarks including Market1501 [43], DukeMTMC-reID [45] and CUHK03 [46], [47]. We compare our PH-GCN with some other state-of-art methods including SSM [35], IDE+CamStyle [37], HA-CNN [6], MGCAM-Siamese [41], Pose-transfer [39], PSE [38], Inception-V1+Open-Pose [13], SGGNN [28] and PCB [11]. We implement our method with two versions, i.e., PH-GCN and PH-GCN+Re-ranking. PH-GCN+Re-ranking further uses re-ranking [33] approach to improve the learning results.

TABLE I: Comparisons results(%) on market1501 dataset on metrics mAP, Rank-1, Rank-5 and Rank-10.

Methods	reference	mAP	Rank-1	Rank-5	Rank-10
SVDNet[3]	ICCV2017	62.1	82.3	92.3	95.2
HydraPlus[32]	ICCV2017	-	76.9	91.3	94.5
PAR[12]	ICCV2017	63.4	81.0	92.0	94.7
PDC* [9]	ICCV2017	63.41	84.14	92.73	94.92
Rerank[33]	CVPR2017	63.63	77.11	-	-
MultiLoss[34]	IJCAI2017	64.4	83.9	-	-
SSM[35]	CVPR2017	68.8	82.21	-	-
DPFL <sup>(2+)</sup> [36]	CHI2017	73.1	88.9	-	-
GLAD(*)[14]	ACM MM2017	73.9	89.9	-	-
IDE+CamStyle[37]	CVPR2018	68.72	88.12	95.1	97.0
+Re-ranking		86.0	91.5	95.0	96.3
PSE [38]	CVPR2018	69.0	87.7	-	-
+Re-ranking		84.0	90.3	-	-
Pose-transfer[39]	CVPR2018	68.92	87.65	-	-
BraidNet-CS+SRL[40]	CVPR2018	69.48	83.7	-	-
MGCAM-Siamese[41]	CVPR2018	74.33	83.79	-	-
SafeNet[42]	IJCAI2018	72.7	90.2	-	-
Inception-V1+OpenPose[13]	ECCV2018	76.0	90.2	96.1	97.4
+Re-ranking		89.9	93.4	96.4	97.4
HA-CNN[6]	CVPR2018	75.7	91.2	-	-
PCB[11]	ECCV2018	77.3	92.4	97.0	97.9
SGGNN[28]	ECCV2018	<b>82.8</b>	92.3	96.1	97.4
<b>PH-GCN</b>		79.0	<b>93.5</b>	<b>97.4</b>	<b>98.5</b>
<b>PH-GCN+Re-ranking</b>		<b>91.1</b>	<b>94.3</b>	<b>97.1</b>	<b>97.8</b>

TABLE II: Comparisons results(%) on DukeMCMT-reID dataset on metrics mAP, Rank-1, Rank-5 and Rank-10.

Methods	reference	mAP	Rank-1	Rank-5	Rank-10
BoW+kissme[43]	ICCV2015	12.2	25.1	-	-
LOMO+XQDA[44]	CVPR2015	17.0	30.8	-	-
SVDNet[3]	ICCV2017	56.8	76.7	-	-
GAN[45]	ICCV2017	47.1	67.7	-	-
PSE [38]	CVPR2018	62.0	79.8	-	-
+Re-ranking		79.8	85.2	-	-
IDE+CamStyle[37]	CVPR2018	53.48	75.27	84.6	87.9
+Re-ranking		73.3	81.4	88.1	90.8
Pose-transfer[39]	CVPR2018	56.49	78.52	-	-
SafeNet[42]	IJCAI2018	57.0	82.7	-	-
BraidNet-CS+SRL[40]	CVPR2018	59.49	76.44	-	-
Inception-V1+OpenPose[13]	ECCV2018	64.2	82.1	90.2	92.7
+Re-ranking		83.9	88.3	93.1	95.0
HA-CNN[6]	CVPR2018	63.8	80.5	-	-
PCB [11]	ECCV2018	65.3	81.9	89.4	91.6
SGGNN[28]	ECCV2018	68.2	81.1	88.4	91.2
<b>PH-GCN</b>		<b>70.7</b>	<b>85.0</b>	<b>92.7</b>	<b>94.8</b>
<b>PH-GCN+Re-ranking</b>		<b>85.7</b>	<b>88.8</b>	<b>93.8</b>	<b>95.9</b>

### A. Datasets and settings

**Market1501** [43] dataset consists of 1501 persons obtained from six camera viewpoints including five high-resolution cameras and one low-resolution camera. It contains 19,732 gallery images and 12,936 training images which are all detected by DPM [48].

**DukeMTMC-reID** [45] dataset is a subset of DukeMTMC dataset [49], which contains 1812 identities observed from 8 different camera viewpoints. It contains 1404 identities, 16522 training images, 2228 queries and 17661 gallery images, respectively.

**CUHK03** [46], [47] dataset contains 13164 images with 1,467 identities. Each identity is observed from two cameras. It contains two kinds of bounding boxes (hand-labeled, DPM-detected) and we use the former one in experiments. We adopt the new training/testing protocol proposed in work [46], [47].

**Evaluation metrics.** Following many previous works [11],

[46], we use Cumulative Matching Characteristic(CMC) at rank-1, rank-5 and rank-10, and the mean average precision (mAP) metrics on all datasets. The mAP is the mean value of average precision across all queries.

### B. Implementation detail

As shown in Figure 1, we use ResNet-50 [29] pre-trained on ImageNet [30] as our backbone network to extract a convolutional feature map for two-stream network, respectively. Then, we use one-layer orthodox convolution and two-layer graph convolutional network respectively to process the deeply learned part features. Finally, the output feature dimension in the perceptron layer is set to 256.

We implement our model with pytorch and training the network on NVIDIA TITAN XP GPUs 12G in an end-to-end manner. All input images are adjusted to a resolution of  $384 \times 128$ , which is the same as that of PCB [11]. Data

augmentation is also adopted for training with horizontal flip, normalization. We set the number of epochs to 60 and the batch size is set as 64 in general for all datasets. We initialize the learning rate of backbone network to 0.1, and set the learning rate of GCN to 0.01 and other layers of network to 1.0. The learning rate is not fixed and begins to decay after 40 epochs. We train the whole network by using stochastic gradient descent (SGD) [50] in each mini-batch.

### C. Comparison results

Table 1-3 summarize the comparison results on Market1501, DukeMTMC-reID and CUHK03 datasets, respectively. The best results are marked by bold. Overall, PH-GCN generally obtains the best results and the re-ranking operation can further improve the performance. More detailedly, we can note that, (1) On Market-1501 dataset, comparing with the baseline model PCB [11], PH-GCN obtains rank-1 = 93.5%, mAP = 79.0%, which have improved performances by 1.7% and 1.1% on metrics mAP and rank-1, respectively. This clearly demonstrates the effectiveness of PH-GCN by further exploiting the structural information of parts. PH-GCN has a higher rank value (rank-1, rank-5 and rank-10 are 1.2%, 1.3% and 1.1% improved) than SGGNN [28] which employs Graph Neural Network (GNN) to guide similarity measurement for Re-ID. (2) On DukeMTMC-reID dataset, compared with PCB [11], PH-GCN results are rank-1 = 85.0% and mAP = 70.7%, which also has 5.4% and 3.1% improvements on mAP and rank-1, respectively. It further demonstrates the effectiveness of our PH-GCN based representation and learning. Compared with SGGNN [28], our result improves 2.5% and 3.9% on mAP and rank-1, respectively. (3) CUHK03 dataset is known to be a very challenging dataset. PH-GCN can still improve 7.3% and 3.6% on mAP and rank-1 when compared with PCB [11]. It further demonstrates the robustness of PH-GCN representation and learning. (4) The re-ranking operation can further consistently improve the performance on all datasets.

### D. Parameter analysis

There exist two balanced parameters  $\epsilon$  (Eq.(2)) and  $\beta$  (Eq.(3)) in PH-GCN. In all experiments, we set  $\{\epsilon, \beta\}$  to  $\{0.75, 0.3\}$ , respectively. Empirically, the proposed model is insensitive to these parameters. When we slightly adjust the parameters, the final Re-ID results only change a little. Figure 2 shows the results of the proposed PH-GCN with different parameters on Market1501 dataset. One can note that, when the parameters are slightly changed, our method maintains good performance, which demonstrates the insensitivity of the proposed method w.r.t. its parameters.

### E. Ablation analysis

In order to further understand and verify the core components (GCN module, hierarchical graph construction) of our PH-GCN model, we conduct ablation analysis experiments on CUHK03 dataset. In particular, to verify the effectiveness of GCN module, we implement a special variant of our model, i.e., Ours-NoGCN that removes GCN module in our PH-GCN network. To demonstrate the benefit of hierarchical

TABLE III: Accuracy comparison on CUHK03 used the new protocol.

Methods	mAP	Rank-1	Rank-5	Rank-10
BoW+kissme [43]	6.4	6.4	-	-
LOMO+XQDA[44]	11.5	12.8	-	-
SVDNet[3]	37.3	41.5	-	-
MGCAM-Siamese[41]	50.21	50.14	-	-
HA-CNN[6]	41.0	44.4	-	-
PCB [11]	54.2	61.3	78.6	85.6
<b>PH-GCN</b>	<b>61.5</b>	<b>64.9</b>	<b>81.8</b>	<b>88.1</b>
<b>PH-GCN+Re-ranking</b>	<b>73.3</b>	<b>70.6</b>	<b>81.9</b>	<b>87.8</b>

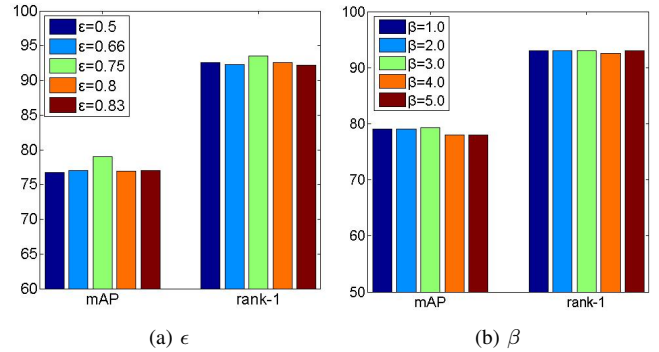


Fig. 2: Results of PH-GCN with different settings of parameters  $\{\epsilon, \beta\}$ .

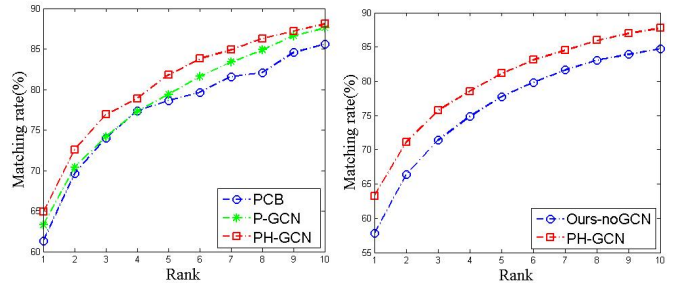


Fig. 3: Performance of two variants (P-GCN, Ours-NoGCN) of the proposed Re-ID model.

graph, we implement a special variant of our model with single layer graph (denoted as P-GCN). As a baseline, we also report the results of PCB [11]. Figure 3 summarizes the comparison results. Here, one can observe that (1) Both PH-GCN and P-GCN obtain better performance than PCB, which demonstrates the effectiveness of the proposed PH-GCN (or P-GCN) by incorporating the inherent spatial relationship information among different parts. (2) PH-GCN performs better than P-GCN, which demonstrates the benefit of hierarchical graph by capturing the structural information of both local and global cues. (3) PH-GCN obviously outperforms Ours-NoGCN, which further shows the desired advantage of the deeply learned context-aware part representation in Re-ID task.

## V. CONCLUSION

This paper proposes a novel Part-based Hierarchical Graph Convolutional Network (PH-GCN) which aims to learn a

hierarchical context-aware part feature representation for person Re-ID problem. PH-GCN also provides a general solution for object (e.g., person) representation and recognition that integrates *local*, *global* and *structural* feature learning simultaneously in a unified end-to-end network. Extensive experiments on three commonly used datasets demonstrate the effectiveness and benefits of the proposed PH-GCN method.

## REFERENCES

- [1] D. Cheng, Y. Gong, S. Zhou, J. Wang, and N. Zheng, "Person re-identification by multi-channel parts-based cnn with improved triplet loss function," in *Computer Vision and Pattern Recognition*, 2016.
- [2] J. Si, H. Zhang, C.-G. Li, J. Kuen, X. Kong, A. C. Kot, and G. Wang, "Dual attention matching network for context-aware feature sequence based person re-identification," in *Proceedings of the IEEE Conference on Computer Vision and Pattern Recognition*, 2018, pp. 5363–5372.
- [3] Y. Sun, L. Zheng, W. Deng, and S. Wang, "Svdnet for pedestrian retrieval," in *IEEE International Conference on Computer Vision*, 2017.
- [4] Y. Shen, H. Li, T. Xiao, S. Yi, D. Chen, and X. Wang, "Deep group-shuffling random walk for person re-identification," in *Proceedings of the IEEE Conference on Computer Vision and Pattern Recognition*, 2018, pp. 2265–2274.
- [5] D. Chen, D. Xu, H. Li, N. Sebe, and X. Wang, "Group consistent similarity learning via deep crf for person re-identification," in *Proceedings of the IEEE Conference on Computer Vision and Pattern Recognition*, 2018, pp. 8649–8658.
- [6] W. Li, X. Zhu, and S. Gong, "Harmonious attention network for person re-identification," in *Proceedings of the IEEE Conference on Computer Vision and Pattern Recognition*, 2018, pp. 2285–2294.
- [7] D. Chen, H. Li, T. Xiao, S. Yi, and X. Wang, "Video person re-identification with competitive snippet-similarity aggregation and co-attentive snippet embedding," in *The IEEE Conference on Computer Vision and Pattern Recognition (CVPR)*, June 2018.
- [8] E. Ustinova, Y. Ganin, and V. Lempitsky, "Multi-region bilinear convolutional neural networks for person re-identification," in *2017 14th IEEE International Conference on Advanced Video and Signal Based Surveillance (AVSS)*. IEEE, 2017, pp. 1–6.
- [9] C. Su, J. Li, S. Zhang, J. Xing, W. Gao, and Q. Tian, "Pose-driven deep convolutional model for person re-identification," in *Proceedings of the IEEE International Conference on Computer Vision*, 2017, pp. 3960–3969.
- [10] A. Schumann and R. Stiefelhofen, "Person re-identification by deep learning attribute-complementary information," in *Proceedings of the IEEE Conference on Computer Vision and Pattern Recognition Workshops*, 2017, pp. 20–28.
- [11] Y. Sun, L. Zheng, Y. Yang, Q. Tian, and S. Wang, "Beyond part models: Person retrieval with refined part pooling (and a strong convolutional baseline)," in *Proceedings of the European Conference on Computer Vision (ECCV)*, 2018, pp. 480–496.
- [12] L. Zhao, X. Li, Y. Zhuang, and J. Wang, "Deeply-learned part-aligned representations for person re-identification," in *The IEEE International Conference on Computer Vision (ICCV)*, Oct 2017.
- [13] Y. Suh, J. Wang, S. Tang, T. Mei, and K. M. Lee, "Part-aligned bilinear representations for person re-identification," in *Computer Vision—ECCV 2018*. Springer, 2018, pp. 418–437.
- [14] L. Wei, S. Zhang, H. Yao, W. Gao, and Q. Tian, "Glad: Global-local-alignment descriptor for pedestrian retrieval," in *Proceedings of the 25th ACM international conference on Multimedia*. ACM, 2017, pp. 420–428.
- [15] F. Zheng, X. Sun, X. Jiang, X. Guo, Z. Yu, and F. Huang, "A coarse-to-fine pyramidal model for person re-identification via multi-loss dynamic training," *arXiv preprint arXiv:1810.12193*, 2018.
- [16] G. Wang, Y. Yuan, X. Chen, J. Li, and X. Zhou, "Learning discriminative features with multiple granularities for person re-identification," *arXiv preprint arXiv:1804.01438*, 2018.
- [17] J. Bruna, W. Zaremba, A. Szlam, and Y. LeCun, "Spectral networks and locally connected networks on graphs," *arXiv preprint arXiv:1312.6203*, 2013.
- [18] T. N. Kipf and M. Welling, "Semi-supervised classification with graph convolutional networks," *arXiv preprint arXiv:1609.02907*, 2016.
- [19] M. Niepert, M. Ahmed, and K. Kutzkov, "Learning convolutional neural networks for graphs," in *International conference on machine learning*, 2016, pp. 2014–2023.
- [20] M. Defferrard, X. Bresson, and P. Vandergheynst, "Convolutional neural networks on graphs with fast localized spectral filtering," in *Advances in neural information processing systems*, 2016, pp. 3844–3852.
- [21] S. Yan, Y. Xiong, and D. Lin, "Spatial temporal graph convolutional networks for skeleton-based action recognition," in *Thirty-Second AAAI Conference on Artificial Intelligence*, 2018.
- [22] J. Bruna, W. Zaremba, A. Szlam, and Y. LeCun, "Spectral networks and locally connected networks on graphs," in *International Conference on Learning Representations*, 2014.
- [23] J. Atwood and D. Towsley, "Diffusion-convolutional neural networks," in *Advances in Neural Information Processing Systems*, 2016, pp. 1993–2001.
- [24] F. Monti, D. Boscaini, J. Masci, E. Rodola, J. Svoboda, and M. M. Bronstein, "Geometric deep learning on graphs and manifolds using mixture model cnns," in *IEEE Conference on Computer Vision and Pattern Recognition*, 2017, pp. 5423–5434.
- [25] P. Veličković, G. Cucurull, A. Casanova, A. Romero, P. Lio, and Y. Bengio, "Graph attention networks," *arXiv preprint arXiv:1710.10903*, 2017.
- [26] M. Guo, E. Chou, D.-A. Huang, S. Song, S. Yeung, and L. Fei-Fei, "Neural graph matching networks for fewshot 3d action recognition," in *Proceedings of the European Conference on Computer Vision (ECCV)*, 2018, pp. 653–669.
- [27] X. Qi, R. Liao, J. Jia, S. Fidler, and R. Urtasun, "3d graph neural networks for rgbd semantic segmentation," in *Proceedings of the IEEE International Conference on Computer Vision*, 2017, pp. 5199–5208.
- [28] Y. Shen, H. Li, S. Yi, D. Chen, and X. Wang, "Person re-identification with deep similarity-guided graph neural network," in *Proceedings of the European Conference on Computer Vision (ECCV)*, 2018, pp. 486–504.
- [29] K. He, X. Zhang, S. Ren, and J. Sun, "Deep residual learning for image recognition," in *The IEEE Conference on Computer Vision and Pattern Recognition (CVPR)*, June 2016.
- [30] O. Russakovsky, J. Deng, H. Su, J. Krause, S. Satheesh, S. Ma, Z. Huang, A. Karpathy, A. Khosla, M. Bernstein *et al.*, "Imagenet large scale visual recognition challenge," *arXiv preprint arXiv:1409.0575*, 2014.
- [31] P.-T. De Boer, D. P. Kroese, S. Mannor, and R. Y. Rubinstein, "A tutorial on the cross-entropy method," *Annals of operations research*, vol. 134, no. 1, pp. 19–67, 2005.
- [32] X. Liu, H. Zhao, M. Tian, L. Sheng, J. Shao, S. Yi, J. Yan, and X. Wang, "Hydraplus-net: Attentive deep features for pedestrian analysis," in *The IEEE International Conference on Computer Vision (ICCV)*, Oct 2017.
- [33] Z. Zhong, L. Zheng, D. Cao, and S. Li, "Re-ranking person re-identification with k-reciprocal encoding," in *The IEEE Conference on Computer Vision and Pattern Recognition (CVPR)*, July 2017.
- [34] W. Li, X. Zhu, and S. Gong, "Person re-identification by deep joint learning of multi-loss classification," *arXiv preprint arXiv:1705.04724*, 2017.
- [35] S. Bai, X. Bai, and Q. Tian, "Scalable person re-identification on supervised smoothed manifold," in *Proceedings of the IEEE Conference on Computer Vision and Pattern Recognition*, 2017, pp. 2530–2539.
- [36] Y. Chen, X. Zhu, and S. Gong, "Person re-identification by deep learning multi-scale representations," in *Proceedings of the IEEE International Conference on Computer Vision*, 2017, pp. 2590–2600.
- [37] Z. Zhong, L. Zheng, Z. Zheng, S. Li, and Y. Yang, "Camera style adaptation for person re-identification," in *Proceedings of the IEEE Conference on Computer Vision and Pattern Recognition*, 2018, pp. 5157–5166.
- [38] M. Saquib Sarfraz, A. Schumann, A. Eberle, and R. Stiefelhofen, "A pose-sensitive embedding for person re-identification with expanded cross neighborhood re-ranking," in *Proceedings of the IEEE Conference on Computer Vision and Pattern Recognition*, 2018, pp. 420–429.
- [39] J. Liu, B. Ni, Y. Yan, P. Zhou, S. Cheng, and J. Hu, "Pose transferrable person re-identification," in *The IEEE Conference on Computer Vision and Pattern Recognition (CVPR)*, June 2018.
- [40] Y. Wang, Z. Chen, F. Wu, and G. Wang, "Person re-identification with cascaded pairwise convolutions," in *Proceedings of the IEEE Conference on Computer Vision and Pattern Recognition*, 2018, pp. 1470–1478.
- [41] C. Song, Y. Huang, W. Ouyang, and L. Wang, "Mask-guided contrastive attention model for person re-identification," in *Proceedings of the IEEE Conference on Computer Vision and Pattern Recognition*, 2018, pp. 1179–1188.
- [42] K. Yuan, Q. Zhang, C. Huang, S. Xiang, C. Pan, and H. Robotics, "Safenet: Scale-normalization and anchor-based feature extraction network for person re-identification," in *IJCAI*, 2018, pp. 1121–1127.
- [43] L. Zheng, L. Shen, L. Tian, S. Wang, J. Wang, and Q. Tian, "Scalable person re-identification: A benchmark," in *The IEEE International Conference on Computer Vision (ICCV)*, December 2015.

- [44] S. Liao, Y. Hu, X. Zhu, and S. Z. Li, "Person re-identification by local maximal occurrence representation and metric learning," in *Proceedings of the IEEE conference on computer vision and pattern recognition*, 2015, pp. 2197–2206.
- [45] Z. Zheng, L. Zheng, and Y. Yang, "Unlabeled samples generated by gan improve the person re-identification baseline in vitro," in *Proceedings of the IEEE International Conference on Computer Vision*, 2017, pp. 3754–3762.
- [46] Z. Zhong, L. Zheng, D. Cao, and S. Li, "Re-ranking person re-identification with k-reciprocal encoding," in *Proceedings of the IEEE Conference on Computer Vision and Pattern Recognition*, 2017, pp. 1318–1327.
- [47] W. Li, R. Zhao, T. Xiao, and X. Wang, "Deepreid: Deep filter pairing neural network for person re-identification," in *CVPR*, 2014.
- [48] P. F. Felzenszwalb, R. B. Girshick, D. McAllester, and D. Ramanan, "Object detection with discriminatively trained part-based models," *IEEE transactions on pattern analysis and machine intelligence*, vol. 32, no. 9, pp. 1627–1645, 2010.
- [49] E. Ristani, F. Solera, R. S. Zou, R. Cucchiara, and C. Tomasi, "Performance measures and a data set for multi-target, multi-camera tracking," *arXiv preprint arXiv:1609.01775*, 2016.
- [50] L. Bottou, "Large-scale machine learning with stochastic gradient descent," in *Proceedings of COMPSTAT'2010*, 2010, pp. 177–186.